ORGANIC LETTERS

2010
Vol. 12, No. 9
2142−2145

Decoding Stereocontrol During the Photooxygenation of Oxazolidinone-Functionalized Enecarbamates

Marissa R. Solomon,[†] J. Sivaguru,[*,‡] Steffen Jockusch,[†] Waldemar Adam,[*,§,⊥] and Nicholas J. Turro[*,†]

Department of Chemistry and Department of Chemical Engineering, Columbia University, 3000 Broadway, New York, New York 10027, Department of Chemistry and Molecular Biology, North Dakota State University, Fargo, North Dakota 58105, Institut für Organische Chemie, Universität Würzburg, 97074 Würzburg, Germany, and Department of Chemistry, University of Puerto Rico, Rio Piedras, PR 00931

njt3@columbia.edu; sivaguru.jayraman@ndsu.edu; wadam@adam.uprr.pr

Received March 19, 2010

ABSTRACT

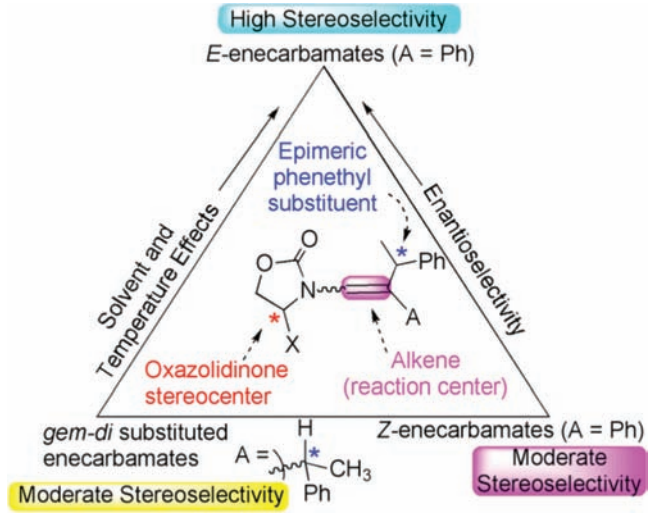

Systematically designed oxazolidinone-derived enecarbamates reveal that solvent and temperature effects on the stereoselectivity during photooxygenation are likely due to the conformational flexibility of the chiral phenethyl side chain (entropy factors); the extent of enantiomeric excess in the photoproduct is dictated by the alkene geometry.

Considering that chirality is integrated into our very survival, it is not remarkable that there is much focus on asymmetric induction and absolute asymmetric synthesis.[1,2] Traditionally, enzymatic and thermal reactions have been employed to

[†] Columbia University.
[‡] North Dakota State University.
[§] Universität Würzburg.
[⊥] University of Puerto Rico.

(1) Miyashita, A.; Yasuda, A.; Takaya, H.; Toriumi, K.; Ito, T.; Souchi, T.; Noyori, R. *J. Am. Chem. Soc.* **1980**, *102*, 7932.
(2) (a) Inoue, Y.; Ramamurthy, V. *Chiral Photochemistry*; Marcel Dekker: New York, 2004. (b) Inoue, Y. *Chem. Rev.* **1992**, *92*, 741. (c) Rau, H. *Chem. Rev.* **1983**, *83*, 535.

10.1021/ol100174r
Published on Web 04/12/2010

achieve high enantioselectivities in asymmetric transformations. Asymmetric photochemistry[2,3] provides an attractive alternative to these traditional routes to produce enantioselectivity. The absorption of light is utilized to generate a short-lived electronically excited state. The stereodifferentiating factors must be able to influence stereoselectivity in the photoproduct within the short lifetime of these excited states.[2,3]

Previously, we demonstrated[4−6] that singlet oxygen ($^1O_2$),[7] an electronically excited molecule, reacts with the oxazolidinone-functionalized enecarbamates **1** to form chiral methyldesoxybenzoin (MDB) as a photoproduct (Scheme 1).

Scheme 1. Photooxygenation of Oxazolidinone-Functionalized Enecarbamate

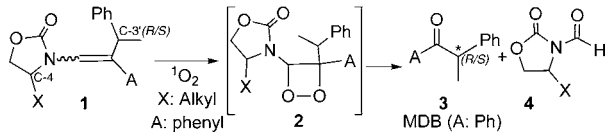

The quite remarkable feature about this system is its stereodifferentiating mechanism (diastereomeric cycloaddition of $^1O_2$ to **1** leading to the formation of the dioxetane **2**; Scheme 1) that results in notable enantiomeric excess (% ee) in the MDB photoproduct with ee values as high as 97%. Furthermore, the stereoselectivity does not depend on the oxazolidinone substituent at the stereogenic C-4 position (Me, ^{i}Pr, or ^{t}Bu give the same stereoselectivity).[4−6] In contrast, the alkene geometry dictates the enantiomeric excess in MDB, with the *E* isomer giving a much larger enantioselectivity than the corresponding *Z* diastereomer.[5,6] Additionally, the *E* enecarbamates are susceptible to solvent and temperature effects, whereas the *Z* diastereomers show no solvent and temperature effects.[5,6]

Given the marked influence of the alkene geometry and the C-3′ phenethyl side chain in the enecarbamates, it was of interest to explore their individual control on the stereochemical outcome during photooxygenation. To decipher the factors responsible for stereoselection, we synthesized the three enecarbamates **1a**−**c** (Scheme 2). We chose the

Scheme 2. Photooxygenation of the Structurally Rich Oxazolidinone-Functionlized Enecarbamates **1a**−**c**

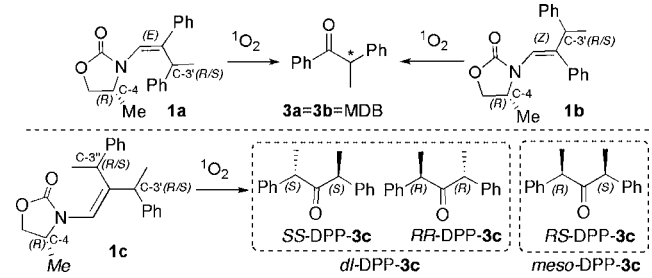

R-configured C-4-methyloxazolidinone chiral auxiliary for all three enecarbamates **1a**−**c**. As established in our previous investigations,[4−6] the stereoselectivity does not depend on the size of this oxazolidinone C-4 substituent. The *E*-**1a** and *Z*-**1b** enecarbamate diastereomers were prepared with phenyl and (*R/S*)-phenethyl substituents at the C-3′ position of the alkene funtionlity. We selected enecarbamate **1c** with two identical *gem*-alkene substituents viz., (*R/S*) phenylethyl substituent at both the C-3′ and C-3″ positions, to eliminate the influence of the alkene geometry on the stereoselectivity in the photooxygenation process (Scheme 2).

Photooxygenation of **1** with $^1O_2$ led to dioxetane **2**, without any noticeable epimerization at the stereogenic centers.[4−6] The dioxetane **2** subsequently decomposed to chiral ketone **3** and the oxazolidinone aldehyde **4** (Scheme 1). In the case of *E*-isomer **1a** and *Z*-isomer **1b**, photooxygenation resulted in the MDB photoproduct **3a** (note that **3a** and **3b** are the same). Similarly, photooxygenation of **1c** (Scheme 2) led to a mixture of *meso*-2,4-diphenyl-3-pentanone *meso*-DPP-**3c**), along with the corresponding *dl* pair (*dl*-DPP **3c**). The DPP photoproduct from enecarbamate **1c** allows determination of both the diastereoselectivity (between the *meso* and *dl* pairs) and enantioselectivity (between the *dl* pairs) as a function of solvent and temperature (Scheme 2).

$$s = (k_R/k_S) = \frac{\ln[1 - c(1 + \text{ee})]}{\ln[1 - c(1 - \text{ee})]} \quad (1)$$

$$\ln(k_R/k_S) = \ln[(100 + \%\ \text{ee})/(100 - \%\ \text{ee})] \quad (2)$$

$$\ln(k_R/k_S) = \Delta\Delta G^{\ddagger} = \Delta\Delta S^{\ddagger}_{R-S}/R - \Delta\Delta H^{\ddagger}_{R-S}/RT \quad (3)$$

Photooxygenation of the enecarbamates **1a**−**c** was performed in three different solvents *viz.*, $CDCl_3$, CD_3OD and CD_3CN at 15−18 °C. The results, tabulated in Table 1, reveal that the *E*-isomer **1a** favors *R*-MDB-**3a** as the photoproduct in $CDCl_3$ and CD_3OD (Table 1; entries 1 and 2), whereas in CD_3CN (Table 1; entry 3) the optical antipode *S*-MDB-**3a**

(3) Griesbeck, A. G.; Kramer, W.; Lex, J. *Angew. Chem., Int. Ed.* **2001**, *40*, 577.

(4) (a) Adam, W.; Bosio, S. G.; Turro, N. J. *J. Am. Chem. Soc.* **2002**, *124*, 14004. (b) Adam, W.; Bosio, S. G.; Turro, N. J. *J. Am. Chem. Soc.* **2002**, *124*, 8814. (c) Adam, W.; Bosio, S. G.; Turro, N. J.; Wolff, B. T. *J. Org. Chem.* **2004**, *69*, 1704. (d) Sivaguru, J.; Poon, T.; Franz, R.; Jockusch, S.; Adam, W.; Turro, N. J. *J. Am. Chem. Soc.* **2004**, *126*, 10816. (e) Sivaguru, J.; Saito, H.; Solomon, M. R.; Kaanumalle, L. S.; Poon, T.; Jockusch, S.; Adam, W.; Ramamurthy, V.; Inoue, Y.; Turro, N. J. *Photochem. Photobiol.* **2006**, *82*, 123. (f) Solomon, M.; Sivaguru, J.; Jockusch, S.; Adam, W.; Turro, N. J. *Photochem. Photobiol. Sci.* **2009**, *8*, 912. (g) Solomon, M.; Sivaguru, J.; Jockusch, S.; Adam, W.; Turro, N. J. *Photochem. Photobiol. Sci.* **2008**, *7*, 531.

(5) Poon, T.; Sivaguru, J.; Franz, R.; Jockusch, S.; Martinez, C.; Washington, I.; Adam, W.; Inoue, Y.; Turro, N. J. *J. Am. Chem. Soc.* **2004**, *126*, 10498.

(6) (a) Sivaguru, J.; Poon, T.; Hooper, C.; Saito, H.; Solomon, M.; Jockusch, S.; Adam, W.; Inoue, Y.; Turro, N. J. *Tetrahedron* **2006**, *62*, 10647. (b) Sivaguru, J.; Saito, H.; Poon, T.; Omonuwa, T.; Franz, R.; Jockusch, S.; Hooper, C.; Inoue, Y.; Adam, W.; Turro, N. J. *Org. Lett.* **2005**, *7*, 2089. (c) Sivaguru, J.; Solomon, M. R.; Saito, H.; Poon, T.; Jockusch, S.; Adam, W.; Inoue, Y.; Turro, N. J. *Tetrahedron* **2006**, *62*, 6707. (d) Sivaguru, J.; Solomon, M. R.; Poon, T.; Jockusch, S.; Bosio, S. G.; Adam, W.; Turro, N. J. *Acc. Chem. Res.* **2008**, *41*, 387.

(7) (a) Foote, C. S. *Acc. Chem. Res.* **1968**, *1*, 104. (b) Wasserman, H. H.; Murray, R. W. *Singlet Oxygen*; Academic: New York, 1979. (c) Frimer, A. A. *Singlet Oxygen*; CRC: Boca Raton, 1985; Vols. 1−4.

Table 1. Solvent Effects during the Photooxygenation of Enecarbamates **1a**−**c**[a−c]

entry	compd	solvent	temp (°C)	% ee (MDB, **3a**)	*s* (MDB, **3a**)
1	**1a**	$CDCl_3$	18	67 (*R*)	5.9
2		CD_3OD	18	75 (*R*)	8.1
3		CD_3CN	18	28 (*S*)	0.5
4	**1b**	$CDCl_3$	15	8 (*R*)	1.4
5		CD_3OD	15	15 (*R*)	2.0
6		CD_3CN	15	5 (*R*)	2.2
entry	compd	solvent	temp (°C)	% ee (*dl*-DPP, **3c**)	*s* (*dl*-DPP-**3c**)
7	**1c**	$CDCl_3$	15	77 (*SS*)	6.3
8		CD_3OD	15	71 (*SS*)	4.8
9		CD_3CN	15	22 (*RR*)	1.8

[a] Concentration of **1a**−**c** = 3.0 mM; sensitizer (methylene blue) = 0.37 mM. [b] The enantiomeric excess (% ee) of the MDB-**3a** and the *dl*-DPP-**3c** photoproducts was determined by GC analysis on a chiral stationary phase (Varian GC3900; Varian CP-Chirasil-Dex CB column). [c] Conversion of enecarbamates (kept below 50%) was determined by GC analysis on an achiral stationary phase (Varian GC3900; Varian Factor-4 VG-1 ms column) or by ^{1}H NMR spectroscopy with 4,4′-di-*tert*-butylbiphenyl as calibration standard. All reported values are an average of a minimum of three runs within 3% error of the stated values. The stereoselectivity factor (*s*), which represents the ratio of the rates of formation (k_R/k_S) of the enantiomeric products, may be computed from the observed ee values at a given conversion by means of eqs 1 and 2 (where *c* = conversion and ee = enantioselectivity in the photoproduct). The *s* factor is a quantitative measure of the relative reaction rates for the two stereoisomers in question corrected for the extent of conversion.

Table 2. Temperature Effects during Photooxygenation of Enecarbamates **1c** in Various Solvents[a−d]

entry	solvent	temp (°C)	% convn	% de	% ee	s (*dl*-DPP-**3c**)
1	$CDCl_3$	15	7	24 (*meso*)	77 (*SS*)	6.3
2		−15	4	12 (*meso*)	89 (*SS*)	14
3		−40	8	10 (*meso*)	90 (*SS*)	16
4	CD_3OD	50	4	19 (*meso*)	68 (*SS*)	6.2
5		15	10	26 (*meso*)	71 (*SS*)	4.8
6		−15	6	24 (*meso*)	76 (*SS*)	4.2
7		−40	5	19 (*meso*)	79 (*SS*)	6.9
8		−78	3	18 (*meso*)	87 (*SS*)	11
9	CD_3CN	50	3	39 (*meso*)	35 (*RR*)	2.7
10		15	19	45 (*meso*)	22 (*RR*)	1.8
11		−15	36	46 (*meso*)	2 (*RR*)	1.8
12		−40	31	42 (*meso*)	1 (*SS*)	1.4

[a] Concentration of **1c** = 3.0 mM; sensitizer (methylene blue) = 0.37 mM. The ratio of epimeric enecarbamate **1c** with fixed C-4(*R*) configuration as determined by ^{1}H NMR spectroscopy was *RS*-5 (1)/*SR*-5 (1.6)/*SS*-5 (0.7)/*RR*-5 (0.6). [b] Conversion (% convn; kept below 50%) was determined by GC analysis on an achiral stationary phase phase (Varian GC3900; Varian Factor-4 VG-1 ms column) or by ^{1}H NMR spectroscopy with 4,4′-di-*tert*-butylbiphenyl as calibration standard. [c] The diastereomeric excess (% de) values were determined by GC analysis (*meso*-DPP-**3c**/*dl*-DPP-**3c**). [d] The enantiomeric excess (% ee) of the *dl*-DPP product **3c** was determined by GC analysis on a chiral stationary phase (Varian GC3900; Varian CP-Chirasil-Dex CB column). All reported values are an average of three runs, reproduced within 3% error of the stated values. Temperature and solvent effects in the case of **1a** and **1b** have been published (refs 5 and 6).

is preferred as the photoproduct. In contrast, the *Z*-isomer **1b** affords *R*-MDB-**3a** irrespective of the employed solvent (Table 1; entries 4−6). In the case of **1c**, the *SS*-DPP-**3c** photoproduct dominated in $CDCl_3$ and CD_3OD (Table 1; entries 7 and 8), while the optical antipode *RR*-DPP-**3c** photoproduct was favored in CD_3CN. For the *gem*-disubstituted enecarbamate **1c** and *E*-enecarbamate **1a**, it is quite striking to observe a similar switch in the enhanced optical antipode of the photoproduct in CD_3CN compared to $CDCl_3$ and CD_3OD.

To ascertain the role of temperature, the photooxygenation of **1c** was carried out at different temperatures in $CDCl_3$, CD_3OD and CD_3CN as listed in Table 2. Inspection of Table 2 reveals that the enantioselectivity between the *dl*-DPP-**3c** depends on the reaction temperature. Two distinct trends are displayed, which in turn depend on the employed solvent. In $CDCl_3$ and CD_3OD, the *ee* values increase upon lowering the temperature, to favor the *SS*-DPP-**3c** enantiomer. In contrast, for CD_3CN, the *ee* values decrease upon lowering the temperature, with the *RR*-DPP-**3c** enantiomer preferred at the higher temperatures of 50 and 15 °C. The enantioselectivity was near zero at the low temperatures of −15 and −40 °C. With respect to diastereoselectivity (*de* values), the *meso*-DPP-**3c** diastereomer was favored over the *dl* pair, irrespective of the solvent and the temperature. Our previous investigation[5,6] with the *E*-isomer **1a** and *Z*-isomer **1b** revealed that the enantioselectivity in the MDB-**3a** photoproduct depends on the temperature and the solvent in the case of the *E* isomer (similar to **1c**), while the *Z* isomer was insensitive to solvent and temperature variations.[5,6] Quite striking are the similar stereoselectivity trends observed upon varying the solvent and temperature during photooxygenation of *E*-**1a** and **1c**.

As we have employed an epimeric mixture of enecarbamates (50:50 mixture of *R/S*-configured phenethyl substituent), the relative reactivity of epimers would dictate the enantioselectivity in the photoproduct. This relative reactivity is empirically defined as the stereoselectivity factor "*s*", given by eq 1[8] That relation exposes the relative rate of formation of the enantiomers from their corresponding diastereomeric transition states of epimeric substrates. Additionally, the stereoselectivity factor "*s*" adjusts for the extent conversion in the photoproduct. A high "*s*" factor ($s > 50$) enables complete kinetic resolution of the photoproduct (at around 50% conversion). We previously demonstrated the practical advantage of high *s* factors, by kinetically resolving the MBD-**3a** enantiomer during the photooxidation of *E*-**1a** with $^1O_2$ (s=72).[5] This implies that in the case of **1c**, for which the maximum *s* factor is 16 in $CDCl_3$ at −40 °C, the maximum ee value of the *dl*-DPP-**3c** photoproduct would be ∼80% at 50% conversions.[8] Thus, complete kinetic resolution of the epimeric enecarbamate **1c** is not feasible.

To understand the solvent and temperature effects in the photooxygenation of **1a**−**c**, the differential activation parameters ($\Delta\Delta S^{\ddagger}_{R\text{-}S}$ and $\Delta\Delta H^{\ddagger}_{R\text{-}S}$) were computed from the

(8) (a) Kagan, H. B.; Fiaud, J. C. *Top. Stereochem.* **1988**, *18*, 249. (b) Keith, J. M.; Larrow, J. F.; Jacobsen, E. N. *Adv. Synth. Catal.* **2001**, *343*, 5.

Eyring plots (Table 3, Figure 1).[9] As may be seen from the eqs 2 and 3, the change in the % ee values (or $\Delta\Delta G^{\ddagger}_{R\text{-}S}$) is enhanced (the $\Delta\Delta S^{\ddagger}$ and $\Delta\Delta H^{\ddagger}$ contributions compensate each other upon temperature variations due to the opposite sign), but in modest preference. As a consequence of the low entropy and enthalpy contributions (as in the case of CD_3OD for **1c**, where the *ee* values increase from 71% at 15 °C to 79% at −40 °C), on decreasing the temperature, the contribution from $\Delta\Delta H^{\ddagger}$ increases slightly. The response to temperature on the enantioselectivity is nominal such that the sense of the enantioselectivity does not change. Thus, the $\Delta\Delta H^{\ddagger}_{R\text{-}S}$ and $\Delta\Delta S^{\ddagger}_{R\text{-}S}$ terms expose the conformational factors.[9] In the present case, presumably, such conformational factors are dictated by the stereogenic center at the C-3′ position of the phenethyl side chain. For substrate **1c** (*gem-di*-substituted alkene), the alkene geometry (*E* or *Z*) cannot exert an influence on the stereoselctivity, such that temperature and solvent effects dominate.

Our investigation of the enecarbamate **1c,** which negates the influence of the alkene geometry due to *gem-di*-substitution, exposes the stereoselectivity of the chiral phenethyl substituent in the photooxidation of *E*-**1a** and *Z*-**1b** enecarbamates (Figure 2). This provides support for our initial suspicion[6] that the greater conformational flexibility of the C-3′ phenethyl substitution is intimately linked to the greater entropic control. This mechanistic insight is pivotal in understanding entropic factors for the design of molecular systems to exploit stereocontrol during light-induced transformations.[10]

Table 3. Activation Parameters $\Delta\Delta H^{\ddagger}$ and $\Delta\Delta S^{\ddagger}$ for the Photooxygenation of **1a**−**c** Enecarbamates[a]

		$\Delta\Delta H^{\ddagger}_{R-S}$ (kcal·mol^{-1})			$\Delta\Delta S^{\ddagger}_{R-S}$ (cal·mol^{-1}·K^{-1})		
entry	solvent	**1a**	**1b**	**1c**	**1a**	**1b**	**1c**
1	$CDCl_3$	−4.9	−0.2	−2.2	−14	0.2	−3.7
2	CD_3OD	−1.5	−0.2	−0.7	−1.0	0.4	0.8
3	CD_3CN	−4.4	−0.1	−1.4	−17	0.1	−6.4

[a] Activation parameters were computed by using eqs 2 and 3 from the data of the Eyring plots.

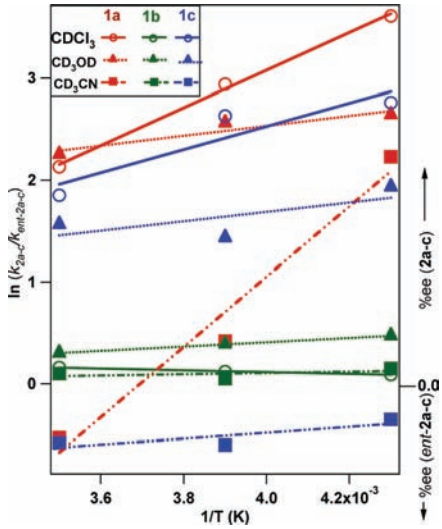

Figure 1. Eyring plot for the photooxygenation of enecarbamates **1a**−**c** (red, **1a**; green, **1b**; blue, **1c**) at various temperatures in $CDCl_3$ (○), CD_3OD (▲), and CD_3CN (■).

depends both on the entropic and enthalpic terms. Since the $\Delta\Delta H^{\ddagger}_{R\text{-}S}/RT$ term is proportional to the reciprocal temperature (eq 3), the $\ln(k_R/k_S)$ value is determined mostly by the enthalpic contribution at low temperatures; however, as the temperature increases, the relative contribution from the $\Delta\Delta S^{\ddagger}_{R\text{-}S}/R$ term increases and begins to override the $\Delta\Delta H^{\ddagger}_{R\text{-}S}/RT$ term at some temperature. Eventually, the sign of the $\ln(k_R/k_S)$ value inverts and the sense of the enantioselectivity switches, provided that the $\Delta\Delta H^{\ddagger}_{R\text{-}S}$ and $\Delta\Delta S^{\ddagger}_{R\text{-}S}$ terms possess the same sign (Table 3). This is the case here for the photooxygenation of the *E*-**1a** and **1c** (e.g., the switch in the chiral sense occurs at −40 °C in CD_3CN for **1c**). In contrast, the corresponding *Z*-**1b** isomer is insensitive to temperature, as convincingly exposed by the near-zero $\Delta\Delta H^{\ddagger}_{R\text{-}S}$ and $\Delta\Delta S^{\ddagger}_{R\text{-}S}$ terms with opposite signs (Table 3; Figure 1 green lines). Consequently, irrespective of what temperature is chosen, the same enantiomeric MDB product

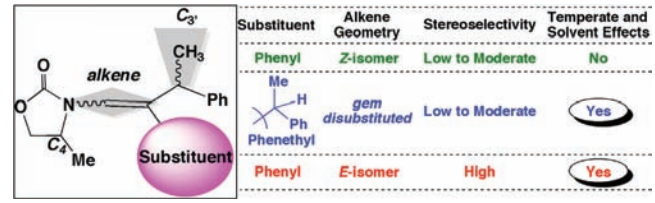

Figure 2. Entropic control and the role of phenethyl substituent during the photooxygenation of **1a**−**c**.

Acknowledgment. The authors at Columbia thank the NSF (CHE-07-17518) for generous support of this research. J.S. (NDSU) thanks the National Science Foundation for generous support through the CAREER award (CHE-0748525). W.A. gratefully acknowledges previous financial support from the Deutsche Forschungsgemeinschaft, Alexander von Humboldt-Stiftung, and the Fonds der Chemischen Industrie.

Supporting Information Available: Synthesis and irradiation procedures and Eyring plots This material is available free of charge via the Internet at http://pubs.acs.org.

OL100174R

(9) (a) Leffler, J. E. *J. Org. Chem.* **1955**, *20*, 1202. (b) Leffler, J. E. *J. Org. Chem.* **1966**, *31*, 533.

(10) (a) Ayitou, A. J.-L.; Jesuraj, J. L.; Barooah, N.; Ugrinov, A.; Sivaguru, J. *J. Am. Chem. Soc.* **2009**, *131*, 11314. (b) Ayitou, A. J.-L.; Sivaguru, J. *J. Am. Chem. Soc.* **2009**, *131*, 5036.